

EPJ B

Condensed Matter
and Complex Systems

EPJ.org

your physics journal

Eur. Phys. J. B (2016) 89: 151

DOI: [10.1140/epjb/e2016-70159-6](https://doi.org/10.1140/epjb/e2016-70159-6)

Bilayer splitting versus Fermi-surface warping as an origin of slow oscillations of in-plane magnetoresistance in rare-earth tritellurides

Pavel D. Grigoriev, Alexander A. Sinchenko, Pascal Lejay, Abdellali Hadj-Azzem, Joël Balay, Olivier Leynaud, Vladimir N. Zverev and Pierre Monceau

 edp sciences



Società Italiana
di Fisica

 Springer

Bilayer splitting versus Fermi-surface warping as an origin of slow oscillations of in-plane magnetoresistance in rare-earth tritellurides

Pavel D. Grigoriev^{1,2,3,*}, Alexander A. Sinchenko^{4,5,6,7}, Pascal Lejay^{6,7}, Abdellali Hadj-Azzem^{6,7}, Joël Balay^{6,7}, Olivier Leynaud^{6,7}, Vladimir N. Zverev^{8,9}, and Pierre Monceau^{6,7}

¹ L.D. Landau Institute for Theoretical Physics, 142432 Chernogolovka, Russia

² National University of Science and Technology “MISIS”, 119049 Moscow, Russia

³ Institut Laue-Langevin, BP 156, 6 rue Jules Horowitz, 38042 Grenoble, France

⁴ Kotel’nikov Institute of Radioengineering and Electronics of RAS, Mokhovaya 11-7, 125009 Moscow, Russia

⁵ National Research Nuclear University (MEPhI), 115409 Moscow, Russia

⁶ Univ. Grenoble Alpes, Inst. Neel, 38042 Grenoble, France

⁷ CNRS, Inst. Neel, 38042 Grenoble, France

⁸ Institute of Solid State Physics, Chernogolovka, 142432 Moscow region, Russia

⁹ Moscow Institute of Physics and Technology, Dolgoprudnyi, 141700 Moscow region, Russia

Received 10 March 2016 / Received in final form 7 May 2016

Published online 15 June 2016 – © EDP Sciences, Società Italiana di Fisica, Springer-Verlag 2016

Abstract. Slow oscillations (SIO) of the in-plane magnetoresistance with a frequency less than 4 T are observed in the rare-earth tritellurides and proposed as an effective tool to explore the electronic structure in various strongly anisotropic quasi-two-dimensional compounds. Contrary to the usual Shubnikov-de-Haas oscillations, SIO originate not from small Fermi-surface pockets, but from the entanglement of close frequencies due to a finite interlayer transfer integral, either between the two Te planes forming a bilayer or between two adjacent bilayers. From the observed angular dependence of the frequency and the phase of SIO we argue that they originate from the bilayer splitting rather than from the Fermi-surface warping. The SIO frequency gives the value of the interlayer transfer integral ≈ 1 meV for TbTe₃ and GdTe₃.

1 Introduction

The measurement of magnetic quantum oscillations (MQO) and angular magnetoresistance oscillations (AMRO) provides a powerful tool to study the electronic properties of various quasi-two-dimensional (Q2D) layered metallic compounds, such as organic metals (see, e.g., Refs. [1–6] for reviews), cuprate and iron-based high-temperature superconductors (see, e.g., [7–16]), heterostructures [17], graphite intercalation compounds [18], etc.

The Fermi surface (FS) of Q2D metals is a cylinder with weak warping $\sim 4t_z/E_F \ll 1$, where t_z is the interlayer transfer integral and $E_F = \mu$ is the in-plane Fermi energy. The MQO with such FS have two close fundamental frequencies $F_0 \pm \Delta F$. In a magnetic field $\mathbf{B} = B_z$ perpendicular to the conducting layers $F_0/B = \mu/\hbar\omega_c$ and $\Delta F/B = 2t_z/\hbar\omega_c$, where $\hbar\omega_c = \hbar eB_z/m^*c$ is the separation between the Landau levels (LL), m^* is an effective electron mass, and c here is the light velocity.

The standard 3D theory of galvanomagnetic properties [19–21] is valid only at $t_z \gg \hbar\omega_c$, being derived in the lowest order in the parameter $\hbar\omega_c/t_z$. This theory predicts several peculiarities of magnetoresistance (MR) in Q2D metals, such as AMRO [22–24] and the beats of MQO amplitude [20]. One can extract the fine details of the FS, such as its in-plane anisotropy [25] and its harmonic expansion [26,27], from the angular dependence of MQO frequencies and from AMRO.

At $t_z \sim \hbar\omega_c$ several new qualitative features of MR appear. At $\hbar\omega_c > t_z$ the strong monotonic growth of longitudinal interlayer MR $R_{zz}(B_z)$ was observed in various Q2D metals [28–37] and explained recently [37–40]. At $t_z \gtrsim \hbar\omega_c$ the MR acquires the so-called slow oscillations [36,41] and the phase shift of beats [41,42]. These two effects are missed by the standard 3D theory [19–21] because they appear in the higher orders in $\hbar\omega_c/t_z$.

These slow oscillations (SIO) originate not from small FS pockets, but from the finite interlayer hopping, because the product of oscillations with two close frequencies $F_0 \pm \Delta F$ gives oscillations with frequency $2\Delta F$. The conductivity, being a non-linear function of the oscillating

* e-mail: grigorev@itp.ac.ru

electronic density of states (DoS) and of the diffusion coefficient, has SIO with frequency $2\Delta F \propto t_z$, while the magnetization, being a linear functional of DoS, does not show SIO [36,41]. The SIO have many interesting and useful features as compared to the fast quantum oscillations. First, they survive at much higher temperature than MQO. Second, they are not sensitive to a long-range disorder, which damps the fast MQO similarly to finite temperature due to a spatial variation of the Fermi energy. Therefore, the Dingle factor and the amplitude of SIO may be much larger than those of usual MQO [36]. Third, the SIO allow to measure the interlayer transfer integral t_z and the in-plane Fermi momentum $p_F \equiv \hbar k_F$. These features make the SIO to be a useful tool to study the electronic properties of Q2D metals [36,41]. Until now, the SIO were investigated only for the *interlayer* conductivity $\sigma_{zz}(B)$, when the current and the magnetic field are both applied perpendicularly to the 2D layers, and only in organic compounds [5,36,41]. At the same time, the most of Q2D compounds, including pnictide high-temperature superconductors, as a rule, have the shape of very thin flakes for which correct measurements of the intralayer conductivity are reliable, especially in the case of good metallic properties of studied compounds.

Very often the crystal consists of a stack of bilayers. In this case there are two types of interlayer hopping integrals: the larger, t_b , is between adjacent layers inside one bilayer, and the smaller one, t_z , is between bilayers. Correspondingly, one may expect two types of SIO originating from the bilayer and interbilayer electron hopping. The SIO from bilayer splitting have not yet been studied.

Below we investigate the possibility and usefulness of SIO in the *intralayer* electrical transport, choosing the non-organic layered Q2D rare-earth tritelluride compounds $R\text{Te}_3$ ($R = \text{Y, La, Ce, Nd, Sm, Gd, Tb, Ho, Dy, Er, Tm}$) as an example. Rare-earth tritellurides have an orthorhombic structure ($Cmcm$) in the normal state and exhibit a c -axis incommensurate charge-density wave (CDW) at high temperature, which was recently a subject of intense studies [43–48]. For the heaviest rare-earth elements, a second a -axis CDW occurs at low temperature. In addition to hosting incommensurate CDWs, magnetic rare-earth ions exhibit closed-spaced magnetic phase transitions below 10 K [49,50] leading to coexistence and competition of many ordered states at low temperatures. Therefore, any information about the Fermi surface on such small energy scale beyond the ARPES resolution [45,51] is very important. An accurate measurement of t_z as function of temperature, provided by SIO, is also useful in these compounds. For the possible observation of the SIO the rare-earth tritellurides are very promising, because they have the appropriate anisotropy and good metallic conductivity up to low temperatures. These compounds well illustrate our goal: in addition to good metallic properties, their available single crystals have a very flat shape, allowing correct measurements of the intralayer conductivity [43]. Note that the $R\text{Te}_3$ compounds have a doubled bilayer crystal structure, since there are two non-equivalent Te bilayers in one elementary cell. Hence, this

compound is a promising candidate for the observation of SIO from bilayer splitting.

2 Experiment

For experiments we have chosen GdTe_3 and TbTe_3 . Single crystals of these compounds were grown by a self-flux technique under purified argon atmosphere as described previously [46]. Thin single crystal samples with a thickness typically 0.1–0.3 μm were prepared by micro-mechanical exfoliation of relatively thick crystals glued on a sapphire substrate. The quality of selected crystals and the spatial arrangement of crystallographic axes were controlled by X-ray diffraction. From high-quality [$R(300\text{ K})/R(10\text{ K}) > 100$] untwinned single crystals we cut bridges with a length 200–500 μm and a width 50–80 μm in well defined, namely [100] and [001], orientations. Contacts for electrical transport measurements in four-probe configuration have been prepared using gold evaporation and cold soldering by In. The resistivity of the TbTe_3 samples typically 0.03 $\text{m}\Omega\text{cm}$ at room temperature was the same as reported in reference [47]. Magnetotransport measurements were performed at different orientations of the magnetic field in the field range up to 9 T using a superconducting solenoid. The field orientation was defined by the angle θ between the field direction and the normal b -axis to the highly conducting (a, c) plane. We used a homemade rotator with an angular accuracy better than 0.1° , having previously allowed to demonstrate the two dimensionality behavior of Bismuth Strontium Calcium Copper Oxide (BSCCO) high T_c superconductors [52]. A great care was made to get rid off any backlash in the rotation.

The magnetoresistance $R(B)$ and its derivative $dR(B)/dB$ as a function of the magnetic field up to $B = 8.2\text{ T}$ applied along the b -axis and with the current applied in the (a, c) plane at $T = 4.2\text{ K}$ are drawn in Figure 1a for GdTe_3 and in Figure 2a for TbTe_3 . For both compounds, oscillations with a very weak amplitude are detectable. At $B > 2\text{ T}$ pronounced Shubnikov-de-Haas (SdH) oscillations with a frequency $F \approx 55\text{--}58\text{ T}$ are observed in dR/dB as seen in the inset of Figure 1a for GdTe_3 . At high field ($B \gtrsim 7\text{ T}$) new oscillations with high frequency ($F \approx 0.7\text{--}0.8\text{ kT}$) appear in TbTe_3 , indicating the existence of several types of pockets on the partially gapped Fermi surface (FS). De Haas-van Alphen oscillations were previously observed [53] from a.c. susceptibility and torque measurements in LaTe_3 with three distinct frequencies $\alpha \sim 50\text{ T}$, $\beta \approx 520\text{ T}$ and $\gamma \sim 1600\text{ T}$. The β frequency was attributed to small FS pockets around the X point in the Brillouin zone, unaffected by the CDW, while the α frequency was assigned to a portion of the reconstructed FS. We can attribute the observed frequency $F \approx 56\text{ T}$ of SdH oscillations above 2 T in GdTe_3 and TbTe_3 similarly to the α frequency in LaTe_3 [53].

However, the more striking result, shown in Figures 1a and 2a, is that, in addition to the rapid SdH oscillations, at low magnetic field ($B < 2\text{ T}$) the magnetoresistance exhibits prominent slow oscillations (SIO) with a very low

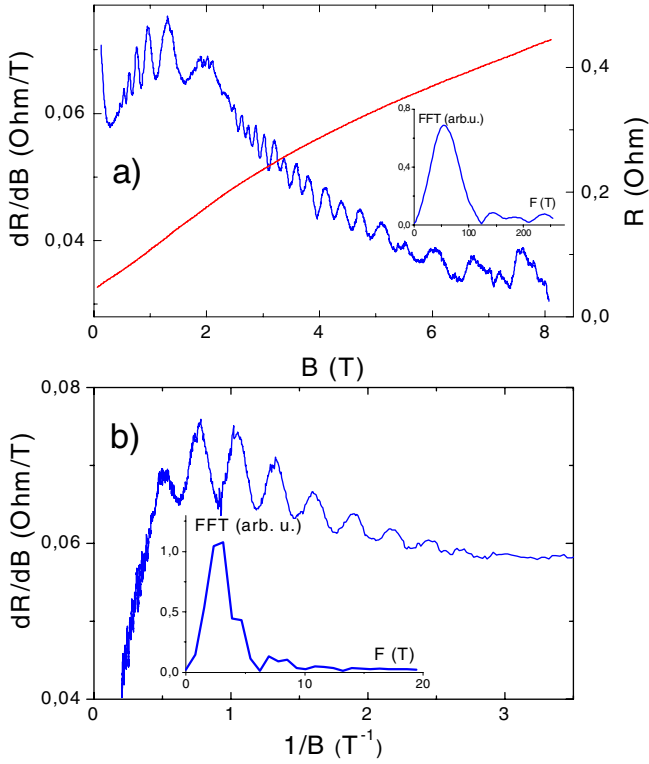


Fig. 1. (a) Magnetoresistance $R(B)$ (red curve) and $dR(B)/dB$ (blue curve) dependencies at 4.2 K of GdTe_3 demonstrating rapid Shubnikov-de-Haas-type oscillations which appear at $B > 2$ T. Inset shows the Fourier transform of Shubnikov-de-Haas oscillations. (b) Variation of $dR(B)/dB$ as a function of the inverse magnetic field, B^{-1} , in the low field range $B < 2$ T demonstrating slow oscillations (SIO). Inset shows the corresponding Fourier transform of SIO.

frequency $F_{slow} \lesssim 4$ T. In Figures 1b and 2b, we have plotted the derivative $dR(B)/dB$ as a function of inverse magnetic field with its Fourier transform (FFT) in the insets. The FFT of slow oscillations and of usual quantum oscillations was done in different magnetic field ranges. Therefore, two peaks of FFT at about 3.5 and 56 T in the spectrum appear only on different plots in Figures 1a and 1b. Below we focus specifically on these slow oscillations.

In contrast to the usual SdH oscillations, the amplitude of which decreases rapidly as temperature increases, the SIO of MR are observable up to $T \simeq 40$ K, as can be seen from Figure 3 where we show the temperature evolution of SIO for GdTe_3 and TbTe_3 . If one extracts the electron effective mass from such weak temperature dependence of SIO amplitude, one obtains $m^* \approx 0.004m_e$, which is unreasonably small. This suggests that the observed SIO originate not from small FS pockets, but from the FS warping due to t_z , similarly to the SIO of interlayer MR in the organic superconductor β -(BEDT-TTF) $_2$ I Br_2 [36], or due to the bilayer splitting t_b . If so, the observed SIO give an excellent opportunity to measure the values of t_b or t_z and k_F at low temperature in rare-earth tritellurides TbTe_3 and GdTe_3 . To discriminate between the two possible origins of SIO, in the next section we consider them in more detail.

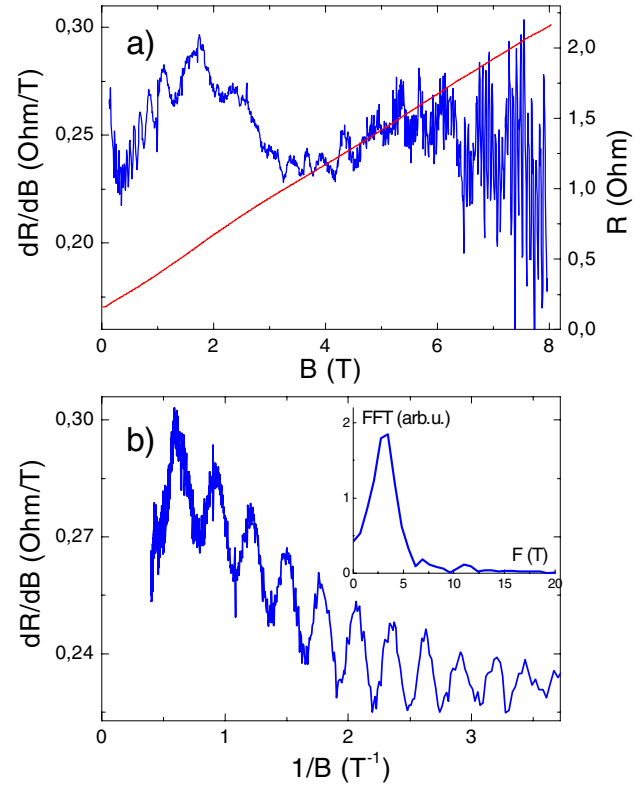


Fig. 2. The same as in Figure 1 for TbTe_3 .

3 Theoretical description

3.1 Slow oscillations of intralayer magnetoresistance due to interlayer dispersion

According to equation (90.5) of reference [54], the intralayer conductivity at finite temperature is given by

$$\sigma_{yy} = e^2 \int d\varepsilon [-n'_F(\varepsilon)] g(\varepsilon) D_y(\varepsilon), \quad (1)$$

where the derivative of the Fermi distribution function $n'_F(\varepsilon) = -1/\{4T \cosh^2[(\varepsilon - \mu)/2T]\}$, $g(\varepsilon)$ is the DoS and $D_y(\varepsilon)$ is the diffusion coefficient of electrons along y -axis. Below one only needs the first terms in the harmonic expansion for the oscillating DoS, which in Q2D metals at finite $t_z \sim \hbar\omega_c$ are given by [41,55–57]

$$g(\varepsilon) \approx g_0 \left[1 - 2 \cos\left(\frac{2\pi\varepsilon}{\hbar\omega_c}\right) J_0\left(\frac{4\pi t_z}{\hbar\omega_c}\right) R_D \right], \quad (2)$$

where $g_0 = m^*/\pi\hbar^2d$ is the DoS at the Fermi level in the absence of magnetic field per two spin components¹, $J_0(x)$ is the Bessel's function, the Dingle factor [61,62] $R_D \approx \exp[-\pi k/\omega_c\tau_0]$, τ_0 is the electron mean free time without magnetic field.

¹ Due to the renormalization of electron spectrum by a CDW even in the mean-field approximation the DoS at the Fermi level may change not so strongly as the FS geometry [58], as observed in ErTe_3 and HoTe_3 [59,60].

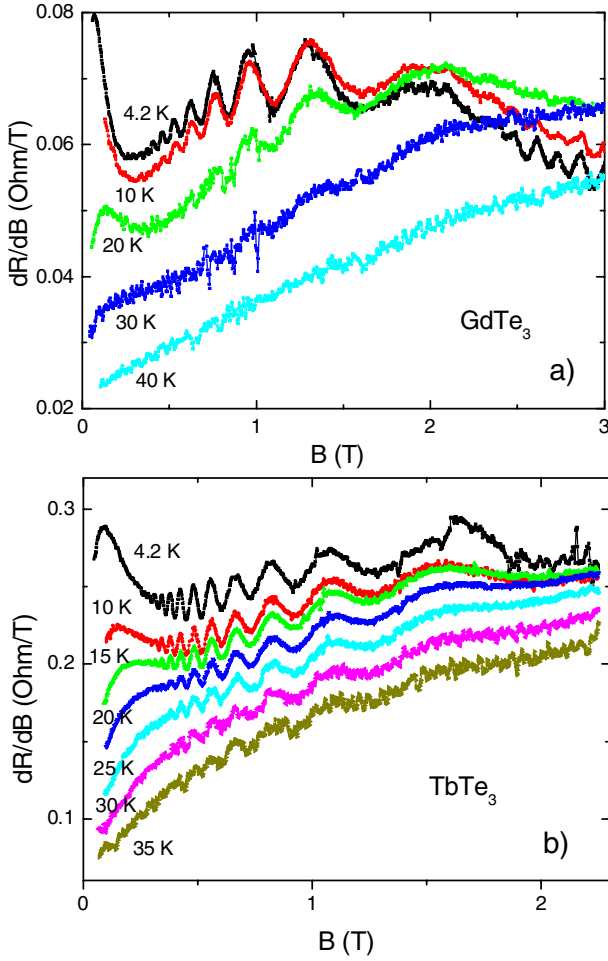


Fig. 3. Temperature evolution of slow oscillations in magnetoresistance for GdTe₃ (a) and TbTe₃ (b).

To calculate the diffusion coefficient² $D_y(\varepsilon)$, we consider only short-range impurities, described by a δ -function potential: $V_i(r) = U\delta^3(r - r_i)$. The matrix element of impurity scattering is given by $T_{mm'} = \Psi_{m'}^*(r_i)U\Psi_m(r_i)$, where $\Psi_m(r)$ is the electron wave function in the state m . During each scattering, the typical change $\Delta y = \Delta P_x c/eB_z$ of the mean electron coordinate y_0 perpendicular to \mathbf{B} is of the order of Larmor radius $R_L = p_{FC}/eB_z$ [63,64]³. The diffusion coefficient is

² The calculation of the diffusion coefficient $D_y(\varepsilon)$ is less trivial than of the DoS and requires to specify the model of disorder. At $\mu \gg \hbar\omega_c$ the quasi-classical approximation is applicable. In an ideal crystal in a magnetic field \mathbf{B} the electrons move along the cyclotron orbits with a fixed center and the Larmor radius $R_L = p_{FC}/eB_z$. Without scattering the electron diffusion in the direction perpendicular to \mathbf{B} is absent. The scattering by impurities changes the electronic states and leads to the electron diffusion.

³ For a short-range disorder the 2D electron wave function in magnetic field decays exponentially at distance larger than the Larmor radius [63,64]. Therefore, for $\Delta y \gg R_L$ the matrix element $T_{mm'}$ is exponentially small resulting from the small overlap of the electron wave functions $\Psi_{m'}^*(r_i)\Psi_m(r_i) \sim \Psi_m^*(r_i + \Delta y)\Psi_m(r_i)$.

approximately given by:

$$D_y(\varepsilon) \approx \langle (\Delta y)^2 \rangle / 2\tau(\varepsilon), \quad (3)$$

where $\tau(\varepsilon)$ is the energy-dependent electron mean scattering time by impurities, and the angular brackets in equation (3) mean averaging over impurity scattering events. In the Born approximation, the mean scattering rate $1/\tau(\varepsilon) = 2\pi n_i U^2 g(\varepsilon)$, where n_i is the impurity concentration. This scattering rate has MQO, proportional to those of the DoS in equation (2). The MQO of $\langle (\Delta y)^2 \rangle \approx R_L^2$ are, usually, weaker and in 3D metals they are neglected [54]. Then $D_y(\varepsilon) \approx R_L^2/2\tau(\varepsilon) \propto g(\varepsilon)$. However, in Q2D metals, when $t_z \sim \hbar\omega_c$, the MQO of $\langle (\Delta y)^2 \rangle$ can be of the same order as the MQO of the DoS, and at $R_D \ll 1$

$$D_y(\varepsilon) \approx D_0 \left[1 - 2\alpha \cos\left(\frac{2\pi\varepsilon}{\hbar\omega_c}\right) J_0\left(\frac{4\pi t_z}{\hbar\omega_c}\right) R_D \right], \quad (4)$$

where $D_0 \approx R_L^2/2\tau_0$, and the number $\alpha \sim 1$. Combining equations (1), (2) and (4) after the integration over ε we obtain

$$\begin{aligned} \frac{\sigma_{yy}(B)}{e^2 g_0 D_0} \approx & 1 + 2\alpha J_0^2(4\pi t_z/\hbar\omega_c) R_D^2 \\ & - 2(\alpha + 1) \cos\left(\frac{2\pi\mu}{\hbar\omega_c}\right) J_0\left(\frac{4\pi t_z}{\hbar\omega_c}\right) R_D R_T, \end{aligned} \quad (5)$$

where the temperature damping factor of the MQO is

$$R_T = (2\pi^2 k_B T / \hbar\omega_c) / \sinh(2\pi^2 k_B T / \hbar\omega_c). \quad (6)$$

The temperature damping factor (6) in the second MQO term in equation (5) arises from the integration over energy ε of the rapidly oscillating function $\propto \cos(2\pi\varepsilon/\hbar\omega_c)$ with the derivative of Fermi distribution function n'_F according to equation (1). The SIO term arises from the ε -independent product $J_0^2(4\pi t_z/\hbar\omega_c)$, and its integration over ε in equation (1) does not produce the temperature damping factor (6). Hence, the SIO, described by the first line of equation (5), are not damped by temperature within our model, similarly to references [36,41].

Approximately, one can use the asymptotic expansion of the Bessel function in equation (5) for large values of the argument: $J_0(x) \approx \sqrt{2/\pi x} \cos(x - \pi/4)$, $x \gg 1$. Then, after introducing the frequency of the SIO, $F_{slow} = 4t_z B/\hbar\omega_c = 4t_z m^* c/e\hbar$, the first line in equation (5) simplifies to:

$$\frac{\sigma_{yy}^{slow}(B)}{e^2 g_0 D_0} \approx 1 + \frac{\alpha \hbar\omega_c}{2\pi^2 t_z} \sin\left(\frac{2\pi F_{slow}}{B}\right) R_D^2. \quad (7)$$

In tilted magnetic field at constant $|\mathbf{B}|$, $\omega_c \propto \cos\theta$ and the angular dependence of interlayer transfer integral is [65]

$$t_z(\theta) = t_z(0) J_0(k_F d \tan\theta), \quad (8)$$

where d is the interlayer distance. Then the frequency of the SIO must depend on the tilt angle θ as:

$$F_{slow}(\theta)/F_{slow}(0) = J_0(k_F d \tan \theta) / \cos(\theta). \quad (9)$$

Equations (8) and (9) assume a single value of the in-plane Fermi momentum k_F . If there are several different FS pockets, the slow oscillations are given by a sum of the contributions from each pocket. Then the simple angular dependence in equation (9) is smeared out, and the deep minima of the SIO frequency $F_{slow}(\theta)$ at the Yamaji angles, observed in reference [36], become weaker or even disappear, being only seen as a splitting or just as a broadening of the Fourier transform peak at certain angles θ . The similar smearing of the simple dependence in equation (9) occurs when the FS pockets are elongated and oriented differently. On the other hand, if the product of interlayer transfer integral t_z and cyclotron mass m^* is the same for all FS pockets, all FS pockets contribute to SIO with the same frequency, which additionally enhances the SIO amplitude as compared to MQO amplitudes. More probable is the case when the SIO frequencies from different FS pockets are close but do not coincide exactly, which enhances but broadens the SIO peak in the Fourier transform of magnetoresistance.

3.2 Slow oscillations due to bilayer splitting

Another possible origin of the slow oscillations comes from the entanglement of two close frequencies due to the bilayer splitting. The elementary crystal cell of RTe₃ in the interlayer z -direction has two conducting Te bilayers separated by insulating RTe slabs (see Fig. 1 in Refs. [51,53]). The interlayer distances are well known for the close compound NdTe₃ [66]. In NdTe₃ the Te layers within one bilayer are separated by a distance of only $d^* \approx 3.64$ Å, and the bilayers are separated by $h \approx 9.26$ Å [66]. As a result the lattice constant $b^* = 2(h + d^*) \approx 25.8$ Å in the interlayer z -direction in RTe₃ is very large. We take these values of d^* , b^* and h for our study of TbTe₃ and GdTe₃.

Assume that the coupling t_z between the bilayers, leading to the interlayer k_z energy dispersion, is negligibly weak, and consider only one bilayer. The interlayer hopping t_b between adjacent layers within one bilayer leads to the so-called bonding and anti-bonding energy states, respectively corresponding to the even and odd electron wave functions in the z -direction. The energy of bonding (even) state is lower than the energy of antibonding (odd) state by the value $\Delta\epsilon \approx 2t_b$. This bilayer splitting is very common also in high-temperature cuprate BSCCO and Yttrium Barium Copper Oxide (YBCO) superconductors, where it has been extensively studied [67–69]. For us it is important only that the in-plane Fermi energy of bonding states is higher than the Fermi energy of antibonding states by this energy splitting $\Delta\epsilon \approx 2t_b$. This results in the corresponding splitting of the basic frequency F_0 of MQO: $F_0 \rightarrow F_0 \pm \Delta F$. Then the DoS is given by a sum of the bonding and antibonding states, and instead of equa-

tion (2) for the DoS we then obtain

$$\frac{g(\epsilon)}{g_0} \approx 1 - R_D \cos\left(2\pi \frac{\epsilon + t_b}{\hbar\omega_c}\right) - R_D \cos\left(2\pi \frac{\epsilon - t_b}{\hbar\omega_c}\right), \quad (10)$$

where g_0 is DoS for two layers (one bilayer). Similarly, instead of equation (4) for the diffusion coefficient we obtain

$$\frac{D_y(\epsilon)}{D_0} \approx 1 - \alpha R_D \left[\cos\left(2\pi \frac{\epsilon + t_b}{\hbar\omega_c}\right) + \cos\left(2\pi \frac{\epsilon - t_b}{\hbar\omega_c}\right) \right]. \quad (11)$$

Instead of equation (5) for the intralayer conductivity from equation (1) one then obtains

$$\begin{aligned} \frac{\sigma_{yy}(B)}{e^2 g_0 D_0} \approx & 1 + \alpha \cos\left(\frac{4\pi t_b}{\hbar\omega_c}\right) R_D^2 \\ & - (\alpha + 1) \cos\left(\frac{2\pi\mu}{\hbar\omega_c}\right) \cos\left(\frac{2\pi t_b}{\hbar\omega_c}\right) R_D R_T. \end{aligned} \quad (12)$$

The SIO, described by the first line of equation (12), are not damped by temperature within our model again, similarly to references [36,41] and equation (5). However, there are several important differences of SIO arising from FS warping and from bilayer splitting. In contrast to the case of FS warping due to k_z dispersion, the frequency of the SIO in the case of bilayer splitting is given by $F_{slow} = 2t_b B / \hbar\omega_c$ not only at $4\pi t_b \gg \hbar\omega_c$ but at any ratio $t_b / \hbar\omega_c$. Also, contrary to equation (7), the SIO amplitude in equation (12) for the case of bilayer splitting does not have the small factor $J_0^2(4\pi t_z / \hbar\omega_c) \sim \hbar\omega_c / 4\pi^2 t_z$. The phase of slow oscillations due to bilayer splitting t_b in equation (12) is shifted by $\pi/2$ as compared to the phase in equation (7) of SIO due to k_z dispersion.

Probably, most evident difference between the SIO due to bilayer splitting and due to k_z dispersion is in the angular dependence of the SIO frequency. This SIO frequency $F_{slow}(\theta)$ does not necessarily obey equation (9) but may have standard cosine dependence $F_{slow}(\theta) = F_{slow}(0) / \cos(\theta)$ [4,5]. Even if one assumes that equation (9) is valid also for the SIO frequency from the bilayer splitting, the interlayer distance d^* in this dependence for

⁴ When SIO originate from the FS warping along z -axis, the angular dependence in equation (9) has an evident geometrical interpretation [23]. This dependence was also confirmed quantum-mechanically using the perturbation theory in the first order in the small parameter $t_z / \hbar\omega_c \ll 1$ [65], and using the double-layer approach and the Feynman diagram technique [70,71]. Hence, by analogy one may assume that equation (9) is also valid for the bilayer splitting. However, this analogy fails in the opposite weak-field regime $t_b / \hbar\omega_c > 1$ when the SIO appear. The geometrical interpretation similar to reference [23], valid in the weak-field regime $t_b / \hbar\omega_c > 1$, is not applicable for bilayer splitting or even gives the standard cosine dependence $F_{slow} \propto 1 / \cos\theta$. Therefore, the problem of the angular dependence of bilayer splitting at arbitrary $t_z / \hbar\omega_c$ and $\omega_c \tau$ needs further theoretical investigation, which is beyond the scope of this paper.

⁵ Equations (8) and (9) assume the spatially uniform interlayer hopping, when the interlayer hopping amplitude t_z does not depend on 2D coordinate within the layer and on in-plane

bilayer splitting is several times smaller than the lattice constant in interlayer z -direction. For example, for RTe_3 compounds the lattice constant in z -direction is $b^* = 25.8 \text{ \AA}$, while the interlayer distance within one bilayer is only $d^* = 3.64 \text{ \AA}$, i.e. 7 times less. Therefore, even according to equation (9), the angular dependence of the frequency $F_{slow}(\theta)$ of SIO originating from the bilayer splitting t_b should be much weaker than that from interbilayer coupling t_z and should start from much higher tilt angle θ .

If there are both types of interlayer coupling, i.e. the transfer integral $t_b = t_b(\mathbf{k}_{\parallel})$ between adjacent layers separated by distance d^* within one bilayer and the hopping $t_z = t_z(\mathbf{k}_{\parallel})$ between adjacent equivalent bilayers, separated by distance h , where \mathbf{k}_{\parallel} is the intralayer momentum, the resulting electron energy spectrum is given by (see, e.g., Eq. (6) of Ref. [68])

$$\epsilon_{\pm}(k_z, \mathbf{k}_{\parallel}) = \epsilon_{\parallel}(\mathbf{k}_{\parallel}) \pm \sqrt{t_z^2 + t_b^2 + 2t_z t_b \cos[k_z(h + d^*)]}. \quad (13)$$

For $t_z \ll t_b$ this equation just gives the double bilayer splitting to bonding and antibonding states. Note, that the derivation of equation (13) assumes [68] that all bilayers are equivalent, i.e. that the lattice constant in z -direction $b^* = h + d^*$. If the bilayers are nonequivalent, as in the case of RTe_3 compounds where $b^* = 2(h + d^*)$, equation (13) needs further modification, which is the subject of separate publication. However, we should notice that if the observed slow oscillations in RTe_3 are due to the coupling t_z between bilayers, in the angular dependence in equations (8) and (9) the distance $h + d^* = b^*/2$ between adjacent bilayers rather than the total lattice constant b^* enters as the interlayer distance d .

4 Discussion

To clarify the origin of the observed SIO, we have experimentally studied the angular dependence of the SIO frequency. The evolution of the SIO in GdTe_3 with the change of the tilt angle θ of magnetic field at $T = 4.2 \text{ K}$ is shown in Figure 4, where the derivative dR/dB is plotted as a function of the perpendicular-to-layers component of the magnetic field $B_{\perp} = B \cos(\theta)$. Note that the magnetic field rotation in the (b, c) and (b, a) planes demonstrated the same results for TbTe_3 .

In Figure 5 we show the θ -dependence of the SIO frequency F_{slow} at $T = 4.2 \text{ K}$ for TbTe_3 (a) and for GdTe_3 (c). The solid curves give the cosine dependence $F(\theta) = F(0)/\cos(\theta)$ typical for MQO. According to equation (9), $F_{slow}(\theta)$ differs from this standard cosine dependence, especially at high tilt angle. In Figure 5b we plot the angular dependence of the product $F_{slow}(\theta) \cos(\theta)$ in TbTe_3 . If the origin of the SIO was due to small FS pockets, the product $F_{slow}(\theta) \cos(\theta)$ would be independent of

electron momentum. If the overlapping atomic orbitals are not uniform but confined within spatial region in the crystalline elementary cell, the simple dependence in equations (8) and (9) may violate, as e.g. in YBCO high-Tc superconductor [68,72].

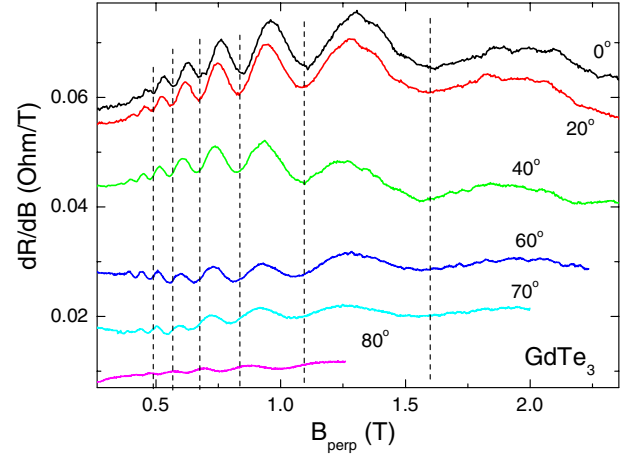


Fig. 4. Slow oscillations observed in GdTe_3 at $T = 4.2 \text{ K}$ for different tilt angles θ between the magnetic field \mathbf{B} and the normal to the conducting layers. $B_{\perp} = B \cos(\theta)$.

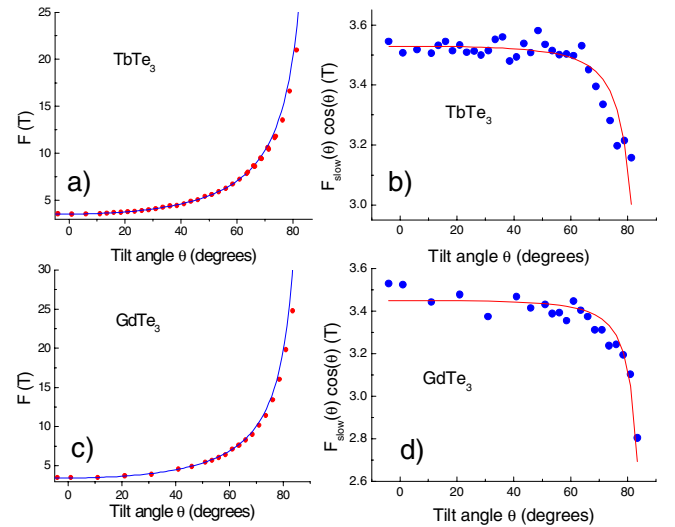


Fig. 5. (a), (c) The frequency of the slow oscillations (SIO) F_{slow} as a function of tilt angle θ at $T = 4.2 \text{ K}$ for TbTe_3 and GdTe_3 . Solid curves show the function $F(\theta) = F(0)/\cos(\theta)$. (b), (d) The angular dependence of the SIO frequency $F_{slow}(\theta)$ in the intralayer magnetoresistance in TbTe_3 and GdTe_3 correspondingly, multiplied by $\cos(\theta)$. The experimental data are shown by blue filled circles, and the theoretical prediction according to equation (9) with $k_F d = 0.12$ for TbTe_3 and $k_F d = 0.11$ for GdTe_3 is shown by solid red lines.

the tilt angle θ . The experimental data, shown by blue filled circles, clearly indicate the deviation from the horizontal line. These experimental data can be reasonably fitted by equation (9) with $k_F d = 0.12$ for TbTe_3 and $k_F d = 0.11$ for GdTe_3 , shown by solid red lines in Figures 5b and 5d. This supports our assertion that the observed slow oscillations originate not from small FS pockets as usual SdH oscillations, but from the entanglement of close frequencies due to a finite interlayer hopping t_z or t_b . Another argument in favor of this origin of the observed SIO is the very weak temperature dependence of their amplitude. To our knowledge, the data obtained

are the first observation of such SIO in the intralayer magnetotransport.

The third argument, supporting the proposed origin of SIO as due to the interlayer hopping rather than due to very small ungapped FS pockets, is that the frequency of the observed SIO is independent of temperature. Indeed, if the observed SIO originated from very small ungapped FS pockets, their frequency would strongly depend on temperature on the scale of the CDW transition temperature, because the size of the ungapped FS pockets depends on the temperature-dependent CDW energy gap. For TbTe₃ the second CDW transition temperature is [73] $T_{c2} = 41$ K, but we do not observe any change in the frequency of SIO up to 35 K (see Fig. 2), which is inconsistent with the small FS-pocket origin of SIO. On contrary, the interlayer transfer integrals t_z or t_b are not sensitive to the in-plane electronic phase transitions and to the in-plane Fermi-surface reconstruction. The interlayer transfer integrals t_z and t_b are determined mainly by the strong (~ 1 eV) crystalline potential in the interlayer direction, which is not affected by the CDW or other in-plane electronic orderings.

According to equation (9), the angular dependence of the frequency $F_{slow}(\theta)$ of SIO allows to estimate the value of the Fermi momentum of the open FS pockets [36]. Fitting the experimental data of $F_{slow}(\theta)$ shown in Figure 5 to equation (9) gives $k_F d \approx 0.11$ for GdTe₃ and $k_F d \approx 0.12$ for TbTe₃. As we showed before, there are two possible origins of the observed SIO in RTe₃: the bilayer splitting t_b and the inter-bilayer coupling t_z . The first double splits the Fermi energy, while the latter leads to the k_z energy dispersion and to the FS warping. Correspondingly, there are two interlayer distances: $d^* \approx 3.64$ Å and $b^*/2 = h + d^* \approx 12.9$ Å. With $d = d^* = 3.64$ Å we obtain $k_F \approx 3.3 \times 10^6$ cm⁻¹, and with $d = b^*/2 = h + d^* \approx 12.9$ Å we obtain $k_F \approx 9.3 \times 10^5$ cm⁻¹. If one assumes that these small FS pockets are not elongated⁶ but almost circular, the corresponding FS cross section areas are $S_{ext} \approx \pi k_F^2$. For the obtained value $k_F \approx 3.3 \times 10^6$ cm⁻¹ for bilayer splitting ($d = d^*$) this gives the MQO frequency $F_0 = S_{ext} \hbar c / 2\pi e \approx 36$ T, a value close to the frequency 55–58 T of oscillations we have measured (inset of Fig. 1a). The difference between the estimated 36 T and the experimental value 55–58 T can be accounted by considering the elongation or another non-circular shape of the FS pockets⁶. Thus, the scenario of the bilayer-splitting origin of SIO looks self-consistent. On the other hand, for the FS warping origin of SIO, taking $d = h + d^*$ and $k_F \approx 9.3 \times 10^5$ cm⁻¹ gives only $F_0 \approx 3$ T. Such a small fundamental frequency of MQO was not measured. Thus the observed angular dependence of SIO frequency suggests that the observed SIO originate from bilayer splitting t_b rather than from FS warping due to t_z .

⁶ Probably, the pockets of the reconstructed FS are elongated and oriented along various directions. Their total contribution to the SIO, being a sum of the contributions from all individual FS pockets, has a smeared angular dependence of the SIO frequency $F_{slow}(\theta)$ as compared to the case of only one elliptical FS pocket observed in β -(BEDT-TTF)₂IBr₂ [36].

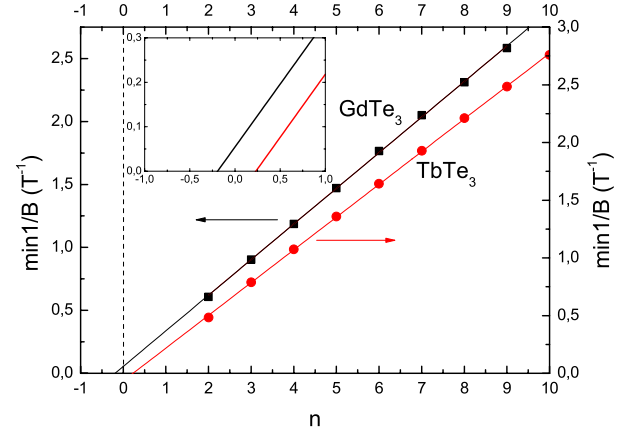


Fig. 6. The measured positions $1/B_{min}$ of the minima in the derivative dR/dB for GdTe₃ (black squares) and TbTe₃ (red circles) at $T = 4.2$ K as function of the number n of these minima. The experimental data are taken from Figures 1 and 2. The solid lines are the best linear fits. Insert figure shows the region around $n = 0$ in a larger scale to emphasize that the fitting lines intersect abscissa axis at $\pm 1/4$.

To further clarify the origin of the observed SIO, we now analyze their phase, which depends on the origin of SIO. In the first scenario, when the SIO originate from the FS warping and interbilayer coupling t_z , the SIO are described by equation (7). At small magnetic field $B < 2$ T, when SIO are observed, the Hall conductivity $\sigma_{xy} \ll \sigma_{yy}$, and the diagonal magnetoresistance $R_{yy} = \sigma_{xx} / (\sigma_{xx} \sigma_{yy} - \sigma_{xy}^2) \approx 1 / \sigma_{yy}$. Then from equation (7) one obtains that the derivative dR/dB , shown in Figures 1b and 2b, is approximately given by:

$$\frac{dR_{yy}^{slow}(B)}{dB} \propto 1 + \frac{\alpha \hbar \omega_c F_{slow}}{\pi t_z B^2} \cos\left(\frac{2\pi F_{slow}}{B}\right) R_D^2, \quad (14)$$

and the position $B_{min,W}(n)$ of the n th minimum of SIO of $dR(B)/dB$ for the warping scenario of SIO is given by

$$F_{slow}/B_{min,W}(n) = n - 1/2. \quad (15)$$

In the second scenario, when SIO originate from the bilayer splitting t_b , one should apply equation (12) instead of equation (7), which gives $R_{yy}(B) \propto 1 - \alpha \cos(2\pi F_{slow}/B) R_D^2$ and

$$\frac{dR_{yy}(B)}{dB} \propto 1 - \alpha \frac{2\pi F_{slow}}{B^2} \sin\left(\frac{2\pi F_{slow}}{B}\right) R_D^2. \quad (16)$$

The position $B_{min,b}(n)$ of the n th minimum of $dR(B)/dB$ in equation (16) is given by

$$F_{slow}/B_{min,b}(n) = n + \text{sign}(\alpha) / 4. \quad (17)$$

The experimental data on the phase of SIO are shown in Figure 6 and can be well fitted by equation (17), corresponding to the bilayer-splitting origin of SIO. On contrary, these data cannot be fitted by equation (15), corresponding to the FS-warping scenario of SIO, originating from the interbilayer coupling t_z . However, it is

not clear why the phase offset $1/4$ in Figure 6 for GdTe_3 and TbTe_3 has different sign, formally corresponding to the different sign of the coefficient α . This difference may, in principle, appear if the reconstructed FS or the parameter $\omega_c\tau$ is considerably different for these two compounds. Therefore, a more rigorous calculation of α in terms of the initial parameters $\omega_c\tau$ and $t_b/\hbar\omega_c$ and detailed experimental data on MQO in these two compounds are needed for understanding this difference.

The observed angular dependence of the frequency $F_{slow}(\theta)$ and the phase of SIO are both in favour of the bilayer-splitting origin of SIO. There is a third argument, supporting this conjecture. If the observed SIO with frequency $F \approx 4$ T were due to FS warping and inter-bilayer hopping t_z , one would expect to observe another SIO with larger frequency, corresponding to the bilayer splitting and the transfer integral $t_b > t_z$. According to equations (7) and (12), the SIO from bilayer splitting should have larger amplitude than SIO from FS warping because of the extra factor $\hbar\omega_c/2\pi^2t_z$ in equation (7) as compared to equation (12). Thus, the second SIO would have even larger amplitude than the observed SIO. However, in experiments there is no any signature of the second SIO, which supports our assertion that the observed SIO originate from the bilayer splitting t_b rather than from FS warping t_z . To our knowledge, the reported results are the first experimental and theoretical study of the slow oscillations of MR originating from the bilayer splitting. However, this phenomenon is expected to be rather general and should be observable in many other bilayered materials.

The SIO of intra- and interlayer electron transport, studied above and in references [36,41], are qualitatively similar and have only some minor quantitative differences in amplitude and phase (compare Eq. (7) above with Eq. (4) of Ref. [36]). On the other hand, the SIO originating from FS warping and from bilayer splitting have qualitative differences, e.g. in the angular dependence of SIO frequency.

The frequency of the SIO at $\theta = 0$ can be used to estimate the value t_b of the interlayer transfer integral. According to equation (7), with the effective electron mass $m^* \approx 0.1m_e$ determined from the temperature dependence of the amplitude of SdH oscillations [74], and $F_{slow} \approx 3.5$ T (see Figs. 5b and 5d), one obtains $t_b \approx 1$ meV. These small values of the interlayer transfer integral t_b in comparison to much larger intralayer transfer integrals $t_{\parallel} \approx 2$ eV along the chains and $t_{\perp} \approx 0.37$ eV perpendicular to the chains in the (a, c) plane, as obtained by the band structure calculations [45], illustrate the quasi-2D character of these rare-earth tritellurides and justify that the dispersion along the b -axis is neglected in ARPES measurements⁷. The value of interlayer transfer

integral t_b is very important for various physical properties of strongly anisotropic compounds. The quantum corrections to conductivity [75,76] rapidly decrease with increasing of t_b , being much stronger in 2D electronic systems. The quantum Hall effect also requires an exponentially small value of interlayer hopping integral [77]⁸.

The proposed technique to measure the electronic structure, namely, the interlayer electron hopping rate and the in-plane Fermi momentum, may be very useful to many other layered materials, including the cuprate and Fe-base high-temperature superconductors. Probably, the quantitative theory of slow oscillations in these materials must include the effects of strong electronic correlations, which are missed in the present one-electron approach⁹. However, the reported first observation and simplified qualitative description of the slow oscillations of the in-plane electronic magnetotransport, as well as their application to extract the electronic-structure parameters of the studied materials, may stimulate further application of this promising technique. The MQO observed in layered high- T_c superconducting materials, usually, have very small amplitudes even in the strongest available magnetic fields, which impedes their application as a tool to study the electronic structure in these materials. The FS reconstruction due to an electronic ordering at finite wave vector, e.g. a density-wave or antiferromagnetic ordering, is known to additionally suppress the MQO because of magnetic breakdown between different FS parts. The SIO, being almost a classical type of magnetoresistance oscillations, do not have these damping factors and can be clearer observed, which enhances their potential use to investigate the electronic structure of various strongly-correlated electronic systems.

To summarize, we report the first observation and qualitative theoretical description of slow oscillations (SIO) of the intralayer magnetoresistance in quasi-2D metallic compounds. These SIO are observed in rather weak magnetic field $B < 2$ T and at rather high temperature up to $T \approx 40$ K, contrary to the usual magnetic quantum oscillations, which are strongly damped by temperature, especially in such weak field. The phase and the angular dependence of the SIO frequency suggest that the observed SIO originate from the bilayer splitting t_b rather than from the FS warping and inter-bilayer hopping t_z , contrary to their origin in the organic metal in reference [36]. Such SIO due to bilayer splitting have not been studied before. The SIO allow to measure the interlayer transfer integral and the in-plane Fermi momentum k_F , which are difficult to measure by other means. We obtained the values $t_b \approx 1$ meV in the rare-earth tritelluride

⁸ A very small interlayer hopping violates the 2D electron localization in the conducting planes by disorder in magnetic field [77], thus preventing the quantum Hall effect.

⁹ Our study raises several important questions, which need further experimental and theoretical investigation. For example, the damping of SIO and of usual MQO amplitudes by the e-e interaction and by critical fluctuations near an electronic phase transition may strongly differ. If so, it may serve as an additional tool to measure these many-particle effects.

⁷ Note that the ARPES measurements do not have a sufficient energy resolution to determine a Fermi-surface reconstruction due to the second low- T_c CDW [45,51]. Therefore, in ARPES data there is no evidence of such small FS pockets. The transport measurements, on contrary, are very sensitive to fine FS details, which is their big advantage as complementary to ARPES technique.

compounds TbTe₃ and GdTe₃. This method is useful to many other layered conductors.

Author contribution statement

A.A. Sinchenko, P. Monceau, and V.N. Zverev performed measurements. P. Lejay, A. Hadj-Azzem, J. Balay, and O. Leynaud prepared the samples. P.D. Grigoriev contributed to theoretical interpretation. All authors participated in the discussion of the results.

The work was partially supported by RFBR (grants Nos. 14-02-01126-a and 16-02-00522-a) and partially performed in the CNRS-RAS Associated International Laboratory between CRTBT and IRE "Physical properties of coherent electronic states in coherent matter".

References

- J. Wosnitza, *Fermi Surfaces of Low-Dimensional Organic Metals and Superconductors* (Springer-Verlag, Berlin, 1996)
- J. Singleton, Rep. Prog. Phys. **63**, 1111 (2000)
- T. Ishiguro, K. Yamaji, G. Saito, *Organic Superconductors*, 2nd edn. (Springer-Verlag, Berlin, 1998)
- The Physics of Organic Superconductors and Conductors*, edited by A.G. Lebed, Springer Series in Materials Science (Springer-Verlag, Berlin, Heidelberg, 2008), Vol. 110
- M.V. Kartsovnik, Chem. Rev. **104**, 5737 (2004)
- M.V. Kartsovnik, V.G. Peschansky, Low Temp. Phys. **31**, 185 (2005) [Fiz. Nizk. Temp. **31**, 249 (2005)]
- N.E. Hussey, M. Abdel-Jawad, A. Carrington, A.P. Mackenzie, L. Balicas, Nature **425**, 814 (2003)
- M. Abdel-Jawad, M.P. Kennett, L. Balicas, A. Carrington, A.P. Mackenzie, R.H. McKenzie, N.E. Hussey, Nat. Phys. **2**, 821 (2006)
- N. Doiron-Leyraud, C. Proust, D. LeBoeuf, J. Levallois, J.-B. Bonnemaïson, R. Liang, D.A. Bonn, W.N. Hardy, L. Taillefer, Nature **447**, 565 (2007)
- M. Abdel-Jawad, J.G. Analytis, L. Balicas, A. Carrington, J.P.H. Charmant, M.M.J. French, N.E. Hussey, Phys. Rev. Lett. **99**, 107002 (2007)
- M.P. Kennett, R.H. McKenzie, Phys. Rev. B **76**, 054515 (2007)
- B. Vignolle, A. Carrington, R.A. Cooper, M.M.J. French, A.P. Mackenzie, C. Jaudet, D. Vignolles, C. Proust, N.E. Hussey, Nature **455**, 952 (2008)
- T. Helm, M.V. Kartsovnik, M. Bartkowiak, N. Bittner, M. Lambacher, A. Erb, J. Wosnitza, R. Gross, Phys. Rev. Lett. **103**, 157002 (2009)
- T. Helm, M.V. Kartsovnik, I. Sheikin, M. Bartkowiak, F. Wolff-Fabris, N. Bittner, W. Biberacher, M. Lambacher, A. Erb, J. Wosnitza, R. Gross, Phys. Rev. Lett. **105**, 247002 (2010)
- Taichi Terashima, Nobuyuki Kurita, Megumi Tomita, Kunihiko Kihou, Chul-Ho Lee, Yasuhide Tomioka, Toshimitsu Ito, Akira Iyo, Hiroshi Eisaki, Tian Liang, Masamichi Nakaïjima, Shigeyuki Ishida, Shin-ichi Uchida, Hisatomo Harima, Shinya Uji, Phys. Rev. Lett. **107**, 176402 (2011)
- D. Graf, R. Stillwell, T.P. Murphy, J.-H. Park, E.C. Palm, P. Schlottmann, R.D. McDonald, J.G. Analytis, I.R. Fisher, S.W. Tozer, Phys. Rev. B **85**, 134503 (2012)
- M. Kuraguchi, E. Ohmichi, T. Osada, Y. Shiraki, Synth. Met. **133-134**, 113 (2003)
- G. Csanyi, P.B. Littlewood, A.H. Nevidomskyy, C.J. Pickard, B.D. Simon, Nat. Phys. **1**, 42 (2005)
- A.A. Abrikosov, *Fundamentals of the Theory of Metals* (North-Holland Publishing, 1988)
- D. Shoenberg, *Magnetic oscillations in metals* (Cambridge University Press, 1984)
- J.M. Ziman, *Principles of the Theory of Solids* (Cambridge University Press, 1972)
- M.V. Kartsovnik, P.A. Kononovich, V.N. Laukhin, I.F. Shchegolev, J. Exp. Theor. Phys. Lett. **48**, 541 (1988)
- K. Yamaji, J. Phys. Soc. Jpn **58**, 1520 (1989)
- R. Yagi, Y. Iye, T. Osada, S. Kagoshima, J. Phys. Soc. Jpn **59**, 3069 (1990)
- M.V. Kartsovnik, V.N. Laukhin, S.I. Pesotskii, I.F. Schegolev, V.M. Yakovenko, J. Phys. I **2**, 89 (1992)
- C. Bergemann, S.R. Julian, A.P. Mackenzie, S. NishiZaki, Y. Maeno, Phys. Rev. Lett. **84**, 2662 (2000)
- P.D. Grigoriev, Phys. Rev. B **81**, 205122 (2010)
- A.I. Coldea, A.F. Bangura, J. Singleton, A. Ardavan, A. Akutsu-Sato, H. Akutsu, S.S. Turner, P. Day, Phys. Rev. B **69**, 085112 (2004)
- R.B. Lyubovskii, S.I. Pesotskii, A. Gilevskii, R.N. Lyubovskaya, J. Exp. Theor. Phys. **80**, 946 (1995) [Zh. Eksp. Teor. Fiz. **107**, 1698 (1995)]
- F. Zuo, X. Su, P. Zhang, J.S. Brooks, J. Wosnitza, J.A. Schlueter, J.M. Williams, P.G. Nixon, R.W. Winter, G.L. Gard, Phys. Rev. B **60**, 6296 (1999)
- J. Hagel, J. Wosnitza, C. Pfeleiderer, J.A. Schlueter, J. Mohtasham, G.L. Gard, Phys. Rev. B **68**, 104504 (2003)
- J. Wosnitza, J. Low Temp. Phys. **146**, 641 (2007)
- M.V. Kartsovnik, P.D. Grigoriev, W. Biberacher, N.D. Kushch, Phys. Rev. B **79**, 165120 (2009)
- W. Kang, Y.J. Jo, D.Y. Noh, K.I. Son, O.-H. Chung, Phys. Rev. B **80**, 155102 (2009)
- J. Wosnitza, J. Hagel, J.S. Qualls, J.S. Brooks, E. Balthes, D. Schweitzer, J.A. Schlueter, U. Geiser, J. Mohtasham, R.W. Winter, G.L. Gard, Phys. Rev. B **65**, 180506(R) (2002)
- M.V. Kartsovnik, P.D. Grigoriev, W. Biberacher, N.D. Kushch, P. Wyder, Phys. Rev. Lett. **89**, 126802 (2002)
- P.D. Grigoriev, M.V. Kartsovnik, W. Biberacher, Phys. Rev. B **86**, 165125 (2012)
- P.D. Grigoriev, Phys. Rev. B **83**, 245129 (2011)
- P.D. Grigoriev, Phys. Rev. B **88**, 054415 (2013)
- A.D. Grigoriev, P.D. Grigoriev, Low Temp. Phys. **40**, 367 (2014) [Fiz. Nizk. Temp. **40**, 472 (2014)]
- P.D. Grigoriev, Phys. Rev. B **67**, 144401 (2003)
- P.D. Grigoriev, M.V. Kartsovnik, W. Biberacher, N.D. Kushch, P. Wyder, Phys. Rev. B **65**, 060403(R) (2002)
- N. Ru, C.L. Condron, G.Y. Margulis, K.Y. Shin, J. Laverock, S.B. Dugdale, M.F. Toney, I.R. Fisher, Phys. Rev. B **77**, 035114 (2008)
- E. DiMasi, M.C. Aronson, J.F. Mansfield, B. Foran, S. Lee, Phys. Rev. B **52**, 14516 (1995)
- V. Brouet, W.L. Yang, X.-J. Zhou, Z. Hussain, R.G. Moore, R. He, D.H. Lu, Z.X. Shen, J. Laverock, S.B. Dugdale, N. Ru, I.R. Fisher, Phys. Rev. B **77**, 235104 (2008)

46. A.A. Sinchenko, P. Lejay, P. Monceau, *Phys. Rev. B* **85**, 241104(R) (2012)
47. A.A. Sinchenko, P.D. Grigoriev, P. Lejay, P. Monceau, *Phys. Rev. Lett.* **112**, 036601 (2014)
48. A.A. Sinchenko, P. Lejay, O. Leynaud, P. Monceau, *Solid State Commun.* **188**, 67 (2014)
49. Y. Iyeiri, T. Okumura, C. Michioka, K. Suzuki, *Phys. Rev. B* **67**, 144417 (2003)
50. N. Ru, J.-H. Chu, I.R. Fisher, *Phys. Rev. B* **78**, 012410 (2008)
51. F. Schmitt, P.S. Kirchmann, U. Bovensiepen, R.G. Moore, J.-H. Chu, D.H. Lu, L. Rettig, M. Wolf, I.R. Fisher, Z.-X. Shen, *New J. Phys.* **13**, 063022 (2011)
52. S. Labdi, S.F. Kim, Z.Z. Li, S. Megtert, H. Raffy, O. Laborde, P. Monceau, *Phys. Rev. Lett.* **79**, 1381 (1997)
53. N. Ru, R.A. Borzi, A. Rost, A.P. Mackenzie, J. Laverock, S.B. Dugdale, I.R. Fisher, *Phys. Rev. B* **78**, 045123 (2008)
54. E.M. Lifshitz, L.P. Pitaevskii, *Course of Theoretical Physics*, in *Physical Kinetics*, 2nd edn. (Nauka, Moscow, 2002), Vol. 10; 1st edn. (Pergamon Press, 1981)
55. V.M. Gvozdkov, *Fiz. Tverd. Tela (Leningrad)* **26**, 2574 (1984) [*Sov. Phys. Solid State* **26**, 1560 (1984)]
56. T. Champel, V.P. Mineev, *Phil. Magazine B* **81**, 55 (2001)
57. T. Champel, V.P. Mineev, *Phys. Rev. B* **66**, 195111 (2002)
58. P.D. Grigoriev, *Phys. Rev. B* **77**, 224508 (2008)
59. R.G. Moore, V. Brouet, R. He, D.H. Lu, N. Ru, J.-H. Chu, I.R. Fisher, Z.-X. Shen, *Phys. Rev. B* **81**, 073102 (2010)
60. F. Pfuner, P. Lerch, J.-H. Chu, H.-H. Kuo, I.R. Fisher, L. Degiorgi, *Phys. Rev. B* **81**, 195110 (2010)
61. R.B. Dingle, *Proc. Roy. Soc. A* **211**, 517 (1952)
62. Yu.A. Bychkov, *Zh. Exp. Theor. Phys.* **39**, 1401 (1960), [*Sov. Phys. J. Exp. Theor. Phys.* **12**, 977 (1961)]
63. M.M. Fogler, A. Yu. Dobin, V.I. Perel, B.I. Shklovskii, *Phys. Rev. B* **56**, 6823 (1997)
64. M.M. Fogler, A.Yu. Dobin, B.I. Shklovskii, *Phys. Rev. B* **57**, 4614 (1998)
65. Yasunari Kurihara, *J. Phys. Soc. Jpn* **61**, 975 (1992)
66. B.K. Norling, H. Steinfink, *Inorg. Chem.* **5**, 1488 (1966)
67. D.L. Feng, N.P. Armitage, D.H. Lu, A. Damascelli, J.P. Hu, P. Bogdanov, A. Lanzara, F. Ronning, K.M. Shen, H. Eisaki, C. Kim, Z.-X. Shen, J.-i. Shimoyama, K. Kishio, *Phys. Rev. Lett.* **86**, 5550 (2001)
68. D. Garcia-Aldea, S. Chakravarty, *New J. Phys.* **12**, 105005 (2010)
69. N. Harrison, B.J. Ramshaw, A. Shekhter, *Sci. Rep.* **5**, 10914 (2015)
70. P. Moses, R.H. McKenzie, *Phys. Rev. B* **60**, 7998 (1999)
71. P.D. Grigoriev, T.I. Mogilyuk, *Phys. Rev. B* **90**, 115138 (2014)
72. O.K. Andersen, A.I. Liechtenstein, O. Jepsen, F. Paulsen, *J. Phys. Chem. Solids* **56**, 1573 (1995)
73. A. Banerjee, Y. Feng, D.M. Silevitch, J. Wang, J.C. Lang, H.-H. Kuo, I.R. Fisher, T.F. Rosenbaum, *Phys. Rev. B* **87**, 155131 (2013)
74. A.A. Sinchenko, P.D. Grigoriev, P. Monceau, P. Lejay, V.N. Zverev, *J. Low Temp. Phys.* (2016), in press, Doi:10.1007/s10909-016-1604-y
75. B.L. Altshuler, A.G. Aronov, *Electron-Electron Interaction In Disordered Conductors*, in *Electron-Electron Interactions in Disordered Systems*, edited by A.L. Efros and M. Pollak (North-Holland, Amsterdam, 1985), Chap. 1
76. M.P. Kennett, R.H. McKenzie, *Phys. Rev. B* **78**, 024506 (2008)
77. B. Huckestein, *Rev. Mod. Phys.* **67**, 357 (1995)